Journal of Hazardous Materials 180 (2010) 79–85

Contents lists available at ScienceDirect

Journal of Hazardous Materials

journal homepage: www.elsevier.com/locate/jhazmat

Dechlorination of pentachlorophenol using nanoscale Fe/Ni particles: Role of nano-Ni and its size effect

Rong Cheng[a], Wei Zhou[b], Jian-Long Wang[a,c,*], Daoduo Qi[d], Lin Guo[b], Wei-Xian Zhang[e], Yi Qian[c]

[a] Laboratory of Environmental Technology, INET, Tsinghua University, Beijing 100084, China
[b] School of Chemistry and Environment Science, Beijing University of Aeronautics and Astronautics, Beijing 100191, China
[c] State Key Joint Laboratory of Environment Simulation and Pollution Control, Tsinghua University, Beijing 100084, China
[d] Department of Environmental Science, Beijing University of Technology, Beijing 100022, China
[e] Department of Civil and Environmental Engineering, Lehigh University, Bethlehem, PA 18015-3176, USA

ARTICLE INFO

Article history:
Received 20 September 2009
Received in revised form 3 March 2010
Accepted 15 March 2010
Available online 23 March 2010

Keywords:
Pentachlorophenol (PCP)
Nanoscale Fe
Nanoscale Ni
Dechlorination
Size effect

ABSTRACT

The dechlorination of pentachlorophenol (PCP) using nano-Fe together with different size of nano-Ni particles (30, 50, 80, and 100 nm) was investigated. The results indicated that nano-Ni particles could improve the dechlorination of PCP. The X-ray powder diffraction (XRD) analysis suggested that nano-Ni particles might serve as catalyst for dechlorination. The decrease of nano-Ni particle size resulted in the increase of PCP transformation and chloride release. The accumulation of several intermediates, such as phenol, 2-chlorophenol, 3-chlorophenol and 4-chlorophenol indicated the probable changes of the reaction pathway for PCP dechlorination. The corrosion products of Fe were detected using XRD analysis. In the system without nano-Ni particles, they were lepidocrocite (γ-FeOOH) and magnetite (Fe_3O_4) and/or maghemite (Fe_2O_3), however, in the systems with nano-Ni particles, they were still magnetite/maghemite but no lepidocrocite existed. The size of nano-Ni particles might affect the crystallization of corrosion products of Fe, but did not affect the species distribution of corrosion products.

1. Introduction

Iron is one of the metals with the richest amount on the earth. As a powerful reducing agent, zero-valent iron (Fe^0) attracted a great deal of attention since 1980s. Because of its easy accessibility, effective degradation for pollutants, generation of very little waste and secondary pollutants, Fe^0 has been widely applied in pollution abatement. Especially in the 1990s, Fe^0 has been used to reduce chlorinated hydrocarbons containing one to two carbon atoms [1–3] and nitrate [4]. Later, nanoscale Fe^0 particles have been synthesized to accelerate reaction rate [5–7]. Compared with their micro-scale counterparts, nanoscale particles offer higher reactivity because of their high specific surface area and high surface reactivity [8]. The nanoparticles can also remain in suspension for extended periods of time to establish an *in situ* treatment zone. Wang and Zhang [9] directly injected nanoscale Fe and Pd/Fe particles into the subsurface as water slurries using gravity flow or moderate injection pressures, the effective treatment of halogenated organic compounds (HOCs) such as trichloroethene (TCE) or polychlorinated biphenyl (PCB) was observed.

Another method used to enhance the Fe^0 activity is through introduction of catalyst. The nanoscale bimetallic particles such as Pd/Fe have been synthesized and evaluated for their reactivity [10–12]. As a precious metal, Pd exhibited excellent catalysis in reductive dechlorination of HOCs by Fe^0. However, high expense of Pd catalyst may restrict its wide application. Similar to Pd, Ni has also been widely used as a catalyst in many fields such as hydrogenation and dehydrogenation of some organic matter [13,14]. Especially, supported Ni has been used for gas phase catalytic hydrodechlorination of chlorinated compounds [15,16]. The introduction of a second catalytic metal could be achieved by several methods, such as the physical mixing of the second metal powder with Fe^0 particles [17,18], the co-reduction of the precursors of the two metals [19], and the post-deposition of the second metal on the surface of Fe^0 particles [2,9,20]. Although some works have been done on the dechlorination ability of Ni/Fe bimetallic particles, there are a few publications about the effect of the size of Ni particles.

Pentachlorophenol (PCP), listed as a priority pollutant by the US EPA, had been used extensively throughout the world as a rice herbicide, wood preservative and general biocide [21]. It is toxic, carcinogenic and refractory [22]. Although the use of PCP has been forbidden, it could persist in the environment for a long time,

* Corresponding author at: Laboratory of Environmental Technology, INET, Tsinghua University, Beijing 100084, China. Tel.: +86 1062784843; fax: +86 1062771150.
E-mail addresses: wangjl@tsinghua.edu.cn, wangjl@mail.tsinghua.edu.cn (J.-L. Wang).

0304-3894/$ – see front matter © 2010 Elsevier B.V. All rights reserved.
doi:10.1016/j.jhazmat.2010.03.068

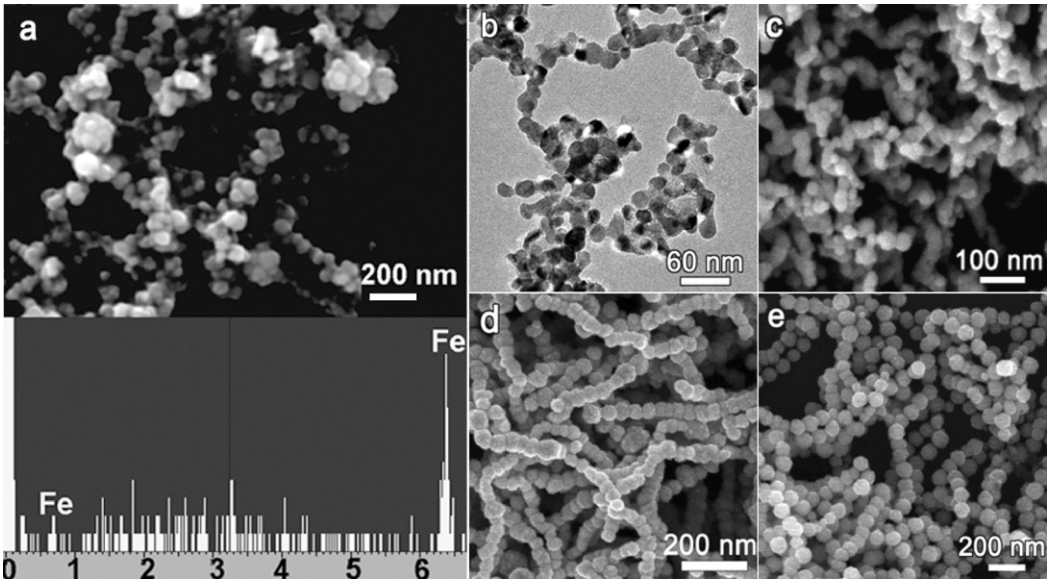

Fig. 1. SEM images and EDS results of Fe and Ni nanoparticles: (a) Fe NPs; Ni NPs with different diameters: (b) 30 nm; (c) 50 nm; (d) 80 nm; (e) 100 nm.

and do harm to human health by bioaccumulation [23]. In an EPA study, PCP was detected in 80% of human urine specimens [21]. Chlorophenols are readily reduced rather than oxidized since they are electronegative. The greater the number of chlorine atoms in the aromatic ring, the more prone the chlorophenols to being reduced than to being oxidized [24].

In this study, PCP was chosen as the target compound. Nanoscale Fe^0 particles were synthesized with potassium borohydride (KBH_4) reduction method [25]. The reactivity of nanoscale Fe^0 and Ni^0 particles for degrading PCP was investigated and the size effect of Ni particles was analyzed. Especially, particles after reaction were characterized by X-ray powder diffraction (XRD).

2. Materials and methods

2.1. Preparation and characterization of nanoparticles

All reagents were analytical grade and used as received. Synthesis of nanoscale Fe^0 particles was achieved by adding 100 ml 0.04 M $FeSO_4{\cdot}7H_2O$ (Shenyang Reagent Factory, Shenyang, China, AR) aqueous solution dropwise to a three-necked flask containing 100 ml 0.2 M KBH_4 (Nankai Fine Chemical Factory, Tianjin, China, AR) aqueous solution at ambient temperature. The process was performed in Ar (Beijing Aolin Gas Company, Beijing, China, AR) atmosphere. Ferric iron was reduced by borohydrate according to the following reaction [26]:

$$Fe(H_2O)_6^{2+} + 2BH_4^- \rightarrow Fe^0\downarrow + 2B(OH)_3 + 7H_2\uparrow \quad (1)$$

Synthesized Fe^0 particles were deposited and then washed with deionized water. The flask was in Ar atmosphere throughout the process.

The morphology of synthesized Fe^0 particles were observed with a scanning electron microscope (SEM, JSM-6301F, JEOL) equipped with energy dispersive spectroscopy (EDS).

Ni^0 nanoparticles (NPs) have been prepared by a mild chemical solution method using PVP as soft templates. Nickel samples with an average diameter of 30, 50, and 80 nm were synthesized by varying the quantities of the reacting and modifying agents, as described in literature [27]. As for the Ni NPs, ~100 nm in diameter, the quantity of $NiCl_2{\cdot}6H_2O$ was increased to 0.238 g, and polyvinyl pyrrolidone (PVP) increased to 0.666 g. They were dissolved in 100 ml ethylene glycol at room temperature. Then 0.5 ml hydrazine monohydrate (80%, v/v) was dropped to the mixture till the color turned into light purple. The stable purple solution was heated to the boiling point of EG (196 °C) and refluxed for 3 h under vigorous magnetic stirring. Finally, the obtained black precipitates were washed with distilled water and ethanol several times.

Field-emission scanning electron microscopy (FE-SEM) was carried out by a field-emission scanning electron microanalyzer (Hitachi S-4800, 5 kV) with the samples obtained in the thick suspension dropping on the silicon slice. The crystal structure of the as-prepared product was characterized by X-ray powder diffraction (XRD) using a Rigaku Dmax 2200 X-ray diffractometer with Cu Kα radiation (λ = 0.1542 nm). The XRD specimens were prepared by flattening the powder on the small slides.

2.2. Experimental procedure

Batch experiments for PCP transformation were conducted in 18 ml bottles. Fifteen mg Fe^0 and 5 mg nano-Ni scale particles were loaded into bottles containing 15 ml of an aqueous solution of PCP. The initial concentration of PCP was 50 mg/l. The bottles were sealed with rubber plugs and placed on a rotary shaker (TZ-2EH, Beijing Wode Company) during the entire experiment period. The temperature of rotary shaker was set to be 30 °C. Parallel control experiments were performed without the nanoscale particles. Each experiment was carried out twice. The standard deviations of duplicate experiments were shown as error bars in figures. All samples were filtrated with 0.45 μm filter film to be analyzed.

2.3. Analysis

PCP samples were analyzed with an Agilent 1200 HPLC (Agilent Ltd.) equipped with an XDB-C^{18} Analytical HPLC column 4.6 × 150 and a 1200 diode-array detector. The mobile phase was 85% methanol and 15% distilled water. The flow rate was 1 ml/min. The detector wavelength was 320 nm. Chlorine ion was measured with a DX-100 ion chromatograph (IC, DIONEX Company, Germany). The operational condition was as follows: eluent at 3.5 mM Na_2CO_3/1.0 mM $NaHCO_3$; eluent flow at 1.2 ml/min, sample loop volume at 250 μl, and run time at 5 min. Deionized water was used as blank. The intermediates and final products of PCP transformation were analyzed with a mass spectrum (MS, P. E API3000) and the HPLC referred above.

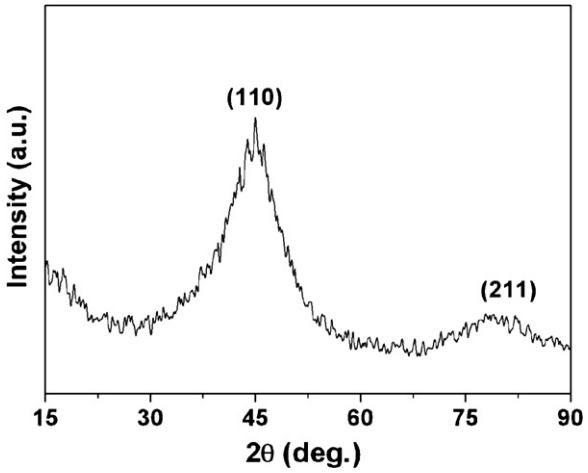

Fig. 2. XRD pattern of synthesized iron particles.

The crystal structure of the particles after reaction was characterized by X-ray powder diffraction (XRD) using a Rigaku D/max-RB X-ray diffractometer with Cu Kα radiation (λ = 0.1542 nm). Scan from $2\theta = 10–90^{\circ}$ was obtained, where θ is the glancing angle between the beam and the sample.

3. Results and discussion

3.1. Characterization of nanoscale particles

The morphology of the nanoscaled particles was shown in Fig. 1. The SEM image in Fig. 1a shows that the diameters of Fe particles were less than 100 nm. Fig. 1b–e shows the overview of the nickel NPs, corresponding to the uniform particles with an average diameter of 30, 50, 80, and 100 nm, respectively. Fig. 2 reveals the XRD pattern for as-synthesized iron particles with zero-valent iron (JCPDS 06-0696). And there are no peaks for oxide phases, indicating the oxidation of the iron particles can be neglected. Fig. 3 shows the phase and purity of the Ni particles with different diameters. All the peaks are well indexed to the diffraction peaks of the planes of $(1\,1\,1)_{Ni}$, $(2\,0\,0)_{Ni}$, and $(2\,2\,0)_{Ni}$ with face centered cubic crystal structure (JCPDS 04-0850). It is obvious that the peaks become broadened as the sample size decrease from 100 to 30 nm.

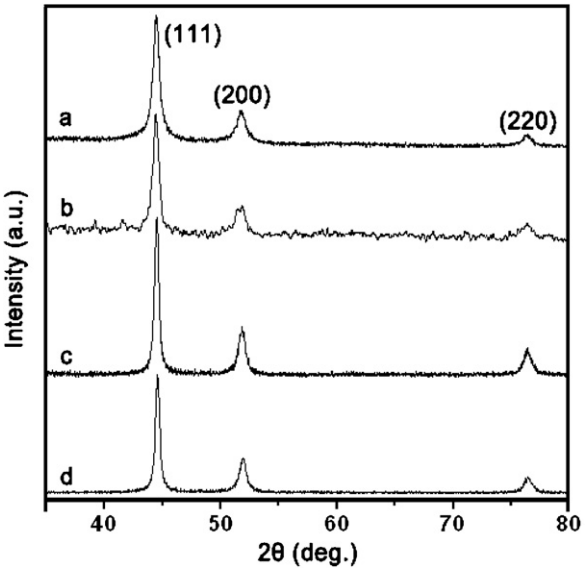

Fig. 3. XRD patterns for the synthesized Ni NPs with different diameters: (a) 30 nm; (b) 50 nm; (c) 80 nm; (d) 100 nm.

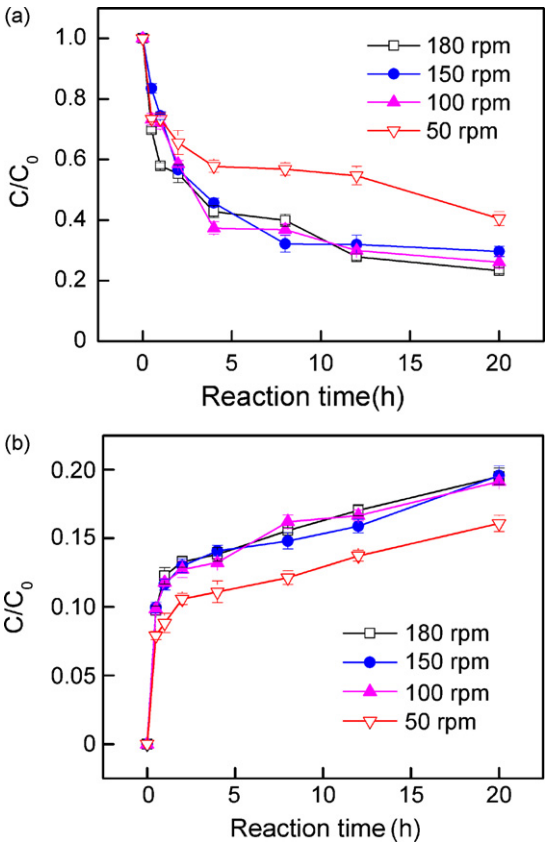

Fig. 4. Removal of PCP and release of Cl^- in the system at different rotary speed. The initial concentration of PCP was 50 mg/l. Metal to solution radio was 15 mg (Fe)/15 ml PCP. (a) PCP removal; (b) Cl^- release.

3.2. Influence of rotary speed

To investigate the influence of mass transport, batch experiments were performed with the speed of rotary shaker being 50, 100, 150, and 180 rpm. The initial pH value of solutions was adjusted to be 8.0. The results were shown in Fig. 4(a). It can be seen that when the speed was 50 rpm, the removal efficiency of PCP was lowest. However, when the speed was over 100 rpm, there was no significant increase of removal efficiency with the increase of rotary speed. The concentration of Cl^- released showed the same trend (Fig. 4(b)). It could be inferred that the rotary speed would affect reaction rate, however, when the speed reached a certain amount, the effect would be negligible.

The reaction process of PCP with Fe nanoparticles could be considered in three steps: the diffusion of Fe and PCP, reaction, the diffusion of products. The rotary speed would mainly affect the diffusion process. When the speed was lower, the diffusion process would take more time. However, when the speed was high enough, the diffusion process was no longer the rate-limiting step. From the results of this study, there would be no significant mass transport limitation when the rotary speed was more than 100 rpm. Similarly, Choe et al. [28] studied reductive denitrification by nanosized Fe^0, and found that the observed reaction rate constant exhibited a linear proportionality with the mixing intensity when the mixing intensity was lower than 40 rpm, the k_{obs} remained almost constant when the mixing intensity was over 40 rpm. In the following experiments, the rotary speed of 150 rpm was used, so the mass transport limitation was negligible during the dechlorination process.

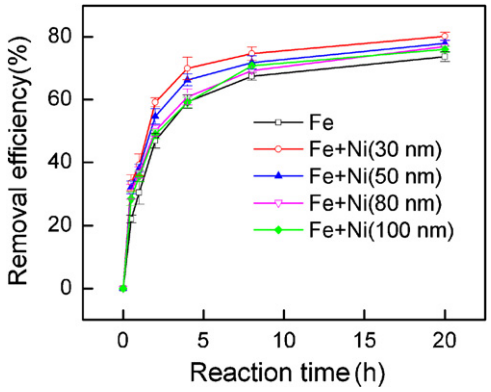

Fig. 5. Transformation of PCP by Fe^0 and Ni^0 nanoparticles. The initial concentration of PCP was 50 mg/l. Metal to solution radio was 15 mg (Fe) + 5 mg (Ni)/15 ml PCP.

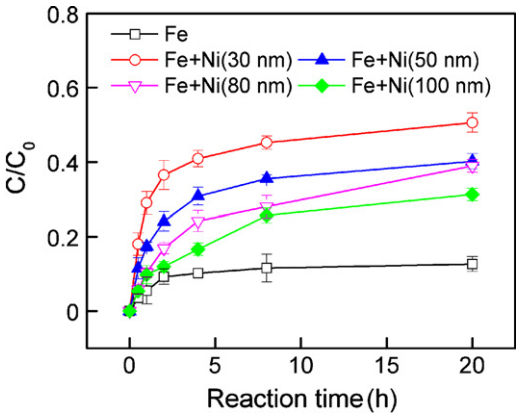

Fig. 6. Cl^- release during the transformation process of PCP by nanoparticles. C_0 is the initial concentration of PCP, and C is concentration of Cl^- in solution.

3.3. Degradation of PCP

Nano-Ni particles of different sizes were physically mixed with Fe nanoparticles to degrade PCP, and quantitative analysis was performed using HPLC. Fig. 5 illustrates the removal efficiency of PCP by different particles. Compared to Fe nanoparticles alone, the presence of nano-Ni particles evidently increased the removal efficiency of PCP. Nano-Ni particles were examined, and the results showed that Ni could not degrade PCP alone (data not shown). So we can infer that Ni particles served as a catalyst (it would be validated in Section 3.6). Moreover, nano-Ni particles could be used for hydrogenation of some organic matter for their favorable storage of hydrogen [13,14,29].

In Fe^0–H_2O systems, the following reaction could take place and hydrogen gas would be produced:

$$Fe^0 + 2H_2O \rightarrow H_2 + 2OH^- + Fe^{2+} \quad (2)$$

Hydrogen is also a good reducing agent, and it can transform organic compounds with some catalyst present [30,31]. As a result, Fe^0 and H_2 could both react with PCP as reducing agents according to the following reactions [32]:

$$Fe^0 + RCl + H_2O \rightarrow Fe^{2+} + RH + Cl^- + OH^- \quad (3)$$

$$H_2 + RCl \rightarrow RH + H^+ + Cl^- \quad (4)$$

Generally speaking, the hydrogen produced is limited, and reaction (4) is not likely to happen when there is not an effective catalyst. However, when the Ni nanoparticles are present, hydrogen can be adsorbed on the surface of Ni and break up into atomic hydrogen. As a powerful reducing agent, the atomic hydrogen on the Ni surface can reduce PCP or its intermediates.

Several researchers used nanoscale Ni/Fe bimetallic particles to degrade the chlorinated hydrocarbons, and obtained similar results [20,33]. However, we used separate Fe and Ni particles instead of Ni/Fe bimetallic particles, which was convenient for controlling the sizes of Ni^0 particles.

As for different size of nano-Ni particles, the results showed that the smaller the particles, the higher the removal efficiency. When the diameter of Ni particles was about 30 nm, the removal efficiency of PCP was about 10% higher than those without nano-Ni particles. While the diameter was about 100 nm, the removal efficiency was about 3% higher. Effect of particle size had been investigated in some fields such as phase transitions [34] and electrochemistry [35,36]. Early in 1982, Plieth [37] studied the electrochemical properties of small metal particles starting with equations for the shift of the reversible redox potential of particles, and gave approximate equations for the relationship between the particle size and the surface charge, the potential of zero charge, the surface potential, work function and quantities related to this function. The results were used to explain the experimental observation in connection with the surface enhanced Raman effect. In our system, Ni served as a catalyst, which was similar to the field of electrochemistry. However, most publications on the pollution abatement paid more attention to the size effect of reactant such as Fe particles, a few researches had been performed on the size effect of catalyst. The results of our experiment revealed that the size effect of catalyst was also an important factor influencing the reaction process.

3.4. Cl^- produced in the system

The relative concentration of Cl^- produced during the process was shown in Fig. 6. It can be seen that much more Cl^- produced in the process with nano-Ni particles than that without Ni particles. And the quantity of Cl^- produced increased evidently with the decrease of Ni particle size. Furthermore, the employ of Ni particles not only promoted the removal of PCP, but promoted the dechlorination of PCP. Considering the probable reactions in the system mentioned above (Section 3.3), it could be inferred that the favorable storage of hydrogen in Ni particles played an important role. And the reduction of PCP by hydrogen should not be ignored in this system. Also, a mass of gas produced during the transformation process was observed. However, whether the gas produced was hydrogen, should be validated in further experiments.

The increase of Cl^- produced with the decrease of Ni particle size could be due to higher capability for storage of hydrogen and stronger catalysis of smaller particles. There was another phenomenon that should be noticed. That is the shift between the removal of PCP and Cl^- produced during the process with Ni particles of different sizes. Take the removal of PCP and Cl^- produced for example, after reacting for 2 h (Fig. 7), the extent of the increase of Cl^- was obviously greater than that of PCP removal. It meant that the ratio of PCP dechlorination to PCP removal increased with the decrease of Ni particle size. The probable explanation could relate to the size effect of nano-Ni particles on the chemical equilibrium, the reaction kinetics and even the reaction mechanisms [38]. Takasu et al. [39] had examined effects of palladium particle size on the electrocatalytic oxidation of carbon monoxide in an acidic solution, and found that the oxidation of carbon monoxide seemed to shift from a one-electron-transfer controlled mechanism to a two-electron-transfer controlled one along with decreasing size of palladium particles. In our system, the specific mechanism has not been defined yet, however, Ni particle size might influence the mechanism according to experimental results.

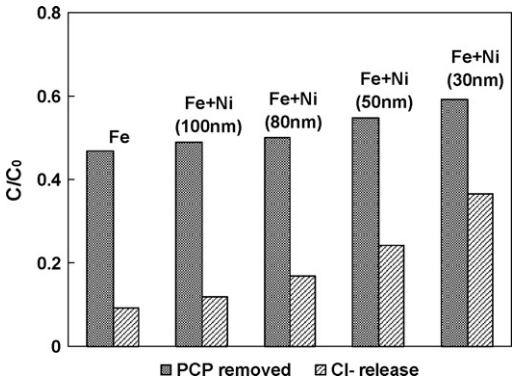

Fig. 7. Removal efficiency of PCP and relative concentration of Cl^- release after reacting for 2 h. C_0 is the initial concentration of PCP, and C is concentration of PCP removed or Cl^- released.

3.5. Intermediates and products of PCP

From the MS results, we can see that PCP was still present in the solution, but it was not the most predominant matter yet. In the solution that reacted for 2 h, chlorinated phenols with four, three, two or one chlorine atoms were all detected. And chlorinated phenols with two chlorine atoms were the most predominant matters. Since there are several isomers for dichlorophenol, we cannot determine which one was the certain matter in the solution from the MS results, or even a mixture of some isomers. The second most predominant matters were chlorophenols. Similarly, there might be a mixture of some chlorophenol (CP) isomers. The HPLC results confirmed the presence of 2-CP, 3-CP, 4-CP and phenol.

Several intermediates such as phenol, 2-CP, 3-CP and 4-CP were quantified through HPLC (Fig. 8). For the systems without Ni particles, there was no phenol detected during reaction period, and the concentrations of 2-CP and 4-CP cumulated were lower than those of systems with Ni present. While the concentration of 3-CP cumulated was not the lowest one. Generally, the concentration of chlorophenols and phenol cumulated in the systems without Ni particles was lower than that of systems with Ni present. Considering the experimental results about removal of PCP and Cl^- released, we can infer that there are more chlorine atoms detached from a molecule of PCP, or there are more intermediates such as tetrachlorophenol, trichlorophenol and dichlorophenol dechlorinated in systems with Ni present. As for phenol cumulated in the systems, there were some fluctuations in the systems with Ni particles of 30, 50, and 80 nm. And the concentration of phenol in system with Ni particles of 100 nm was growing. That means phenol was not the final product, and the degradation rate of phenol in systems with smaller Ni particles was higher. And for 2-CP, the peak was delayed in the systems with Ni particles present. The trend of 4-CP cumulated is similar, but the peak in systems with Ni particles present was much higher. And for 3-CP, the peak was ahead or delayed in the systems with Ni particles present. And there was not a similar variation tendency between any of the five systems. In a word, the present of Ni nanoparticles changed the dechlorination route of chlorinated phenols in the systems, including PCP and its intermediates. However, there are several kinds of chlorinated phenols in the systems, and further determination on the other intermediates is still needed.

For a certain system, the concentration of chlorophenols cumulated followed this order: 2-CP > 4-CP > 3-CP, though the concentration of 3-CP and 4-CP was very close after reacting for 4 h in the system without Ni particles. In the early study we carried out on degradation of chlorophenols by nanoscale Fe^0, the degradation rate of chlorophenols followed the order: 2-CP > 3-CP > 4-CP [40]. So we can infer that there were more 2-CP produced during the reaction.

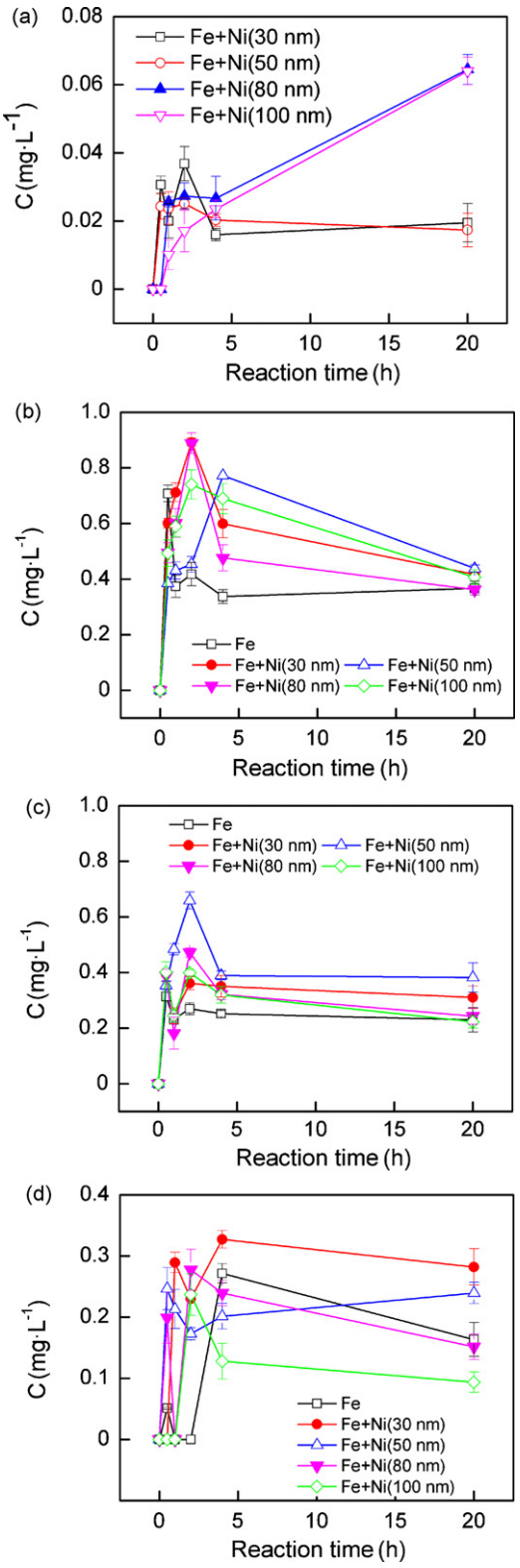

Fig. 8. Some intermediates accumulated in different systems: (a) phenol; (b) 2-CP; (c) 4-CP; (d) 3-CP.

3.6. Transformation of metal particles

The particles after reaction were examined by XRD (Fig. 9), and the analysis results indicated the presence of magnetite (Fe_3O_4) and/or maghemite (Fe_2O_3) in all samples. Because magnetite and maghemite are isostructural, and were effectively indistinguish-

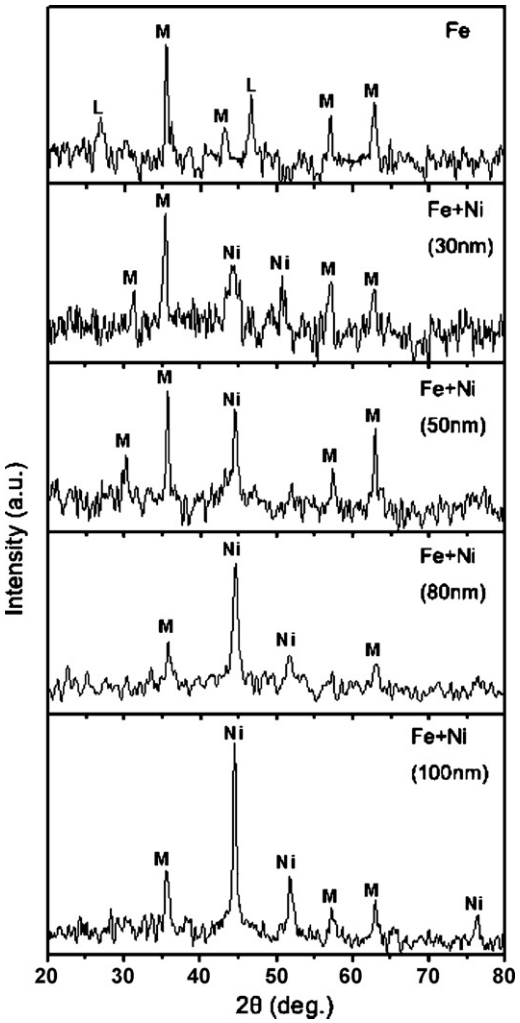

Fig. 9. XRD spectrum of the particles after reacting with different nanoparticles. Major peaks are due to magnetite/maghemite (M), lepidocrocite (L) and pure Ni^0.

able by our XRD data, either oxide may be present. In the system without nano-Ni particles, the XRD analysis indicated the presence of lepidocrocite (γ-FeOOH) as well as magnetite and/or maghemite. Similar results were reported in corrosion products from As removal by nanoscale or common Fe^0 [41,42]. Besides, Gu et al. [43] had also found these phases as well as akaganeite (β-FeOOH) and goethite (α-FeOOH) in Fe^0 corrosion products from column studies. Lepidocrocite, magnetite and maghemite were corrosion products of iron. These Fe(II)/(III) and Fe(III) corrosion products indicated that Fe(II) formation was an intermediate step in the transformation process.

As for reactions with both Fe^0 and Ni^0 nanoparticles in the system, the XRD patterns indicated all the diffraction peaks can be indexed to the pure Ni with face centered cubic crystal structure (JCPDS 04-0850). There were no peaks of lepidocrocite detected in these samples, and the broadness of magnetite (Fe_3O_4) and/or maghemite (Fe_2O_3) was changed. The size of nano-Ni particles might affect the crystallization of corrosion products of Fe to a certain extent. But there were no changes for the species distributing of corrosion products.

4. Conclusions

PCP could be effectively transformed by Fe nanoparticles. The addition of nano-Ni particles could improve the removal of PCP and Cl^- release. However, nano-Ni particles could not degrade PCP alone. This results together with the XRD analysis of particles after reaction suggested that nano-Ni particles served as catalysts. Along with the decrease of Ni particle size, both the removal efficiency of PCP and Cl^- release increased. The accumulation of some intermediates, such as phenol, 2-CP, 3-CP and 4-CP changed when Ni nanoparticles was present. And it indicated some changes of reaction routes.

Lepidocrocite (γ-FeOOH) and magnetite (Fe_3O_4) and/or maghemite (Fe_2O_3) were corrosion products of Fe according to XRD analysis of particles after reaction in the system without Ni particles. Considering probable reactions in the system, these Fe(II)/(III) and Fe(III) corrosion products indicated that Fe(II) formation was an intermediate step in the transformation process. In the systems with nano-Ni particles, no peaks of lepidocrocite were detected. The size of nano-Ni particles might affect the crystallization of corrosion products of Fe, but did not affect the species distribution of corrosion products.

Acknowledgements

This work was supported by the National Natural Science Foundation of China (Grant No. 50928802) and the China Postdoctoral Science Foundation (Grant No. 20090450027), which are greatly acknowledged.

References

[1] R.W. Gillham, S.F. O'Hannesin, Enhanced degradation of halogenated aliphatics by zero-valent iron, Ground Water 32 (1994) 958–967.
[2] R. Muftikian, Q. Fernando, N. Korte, A method for the rapid dechlorination of low molecular weight chlorinated hydrocarbons in water, Water Res. 29 (1995) 2434–2439.
[3] A.L. Roberts, L.A. Totten, W.A. Arnold, D.R. Burris, T.J. Campbell, Reductive elimination of chlorinated ethylenes by zero-valent metals, Environ. Sci. Technol. 30 (1996) 2654–2659.
[4] C.P. Huang, H.W. Wang, P.C. Chiu, Nitrate reduction by metallic iron, Water Res. 32 (1998) 2257–2264.
[5] S. Choe, S.H. Lee, Y.Y. Chang, K.Y. Hwang, J. Khim, Rapid reductive destruction of hazardous organic compounds by nanoscale Fe^0, Chemosphere 42 (2001) 367–372.
[6] B. Schrick, B.W. Hydutsky, J.L. Blough, T.E. Mallouk, Delivery vehicles for zerovalent metal nanoparticles in soil and groundwater, Chem. Mater. 16 (2004) 2187–2193.
[7] T. Phenrat, N. Salen, K. Sirk, R.D. Tilton, G. Lowry, Aggregation and sedimentation of aqueous nanoscale zerovalent iron dispersions, Environ. Sci. Technol. 41 (2007) 284–290.
[8] J.T. Nurmi, P.G. Tratnyek, V. Sarathy, D.R. Baer, J.E. Amonette, K. Pecher, C. Wang, J.C. Linehan, D.W. Matson, R.L. Penn, M.D. Driessen, Characterization and properties of metallic iron nanoparticles: spectroscopy, electrochemistry, and kinetics, Environ. Sci. Technol. 39 (2005) 1221–1230.
[9] C.B. Wang, W.X. Zhang, Synthesizing nanoscale iron particles for rapid and complete dechlorination of TCE and PCBs, Environ. Sci. Technol. 31 (1997) 2154–2156.
[10] T. Li, J. Farrell, Reductive dechlorination of trichloroethene and carbon tetrachloride using iron and palladized-iron cathodes, Environ. Sci. Technol. 34 (2000) 173–179.
[11] D.W. Elliott, W.X. Zhang, Field assessment of nanoscale biometallic particles for groundwater treatment, Environ. Sci. Technol. 35 (2001) 4922–4926.
[12] J. Feng, T.T. Lim, Iron-mediated reduction rates and pathways of halogenated methanes with nanoscale Pd/Fe: analysis of linear free energy relationship, Chemosphere 66 (2007) 1765–1774.
[13] Y. Du, H.L. Chen, R.Z. Chen, N.P. Xu, Synthesis of p-aminophenol from p-nitrophenol over nano-sized nickel catalysts, Appl. Catal. A: Gen. 277 (2004) 259–264.
[14] R. Wojcieszak, M. Zielinski, S. Monteverdi, M.M. Bettahar, Study of nickel nanoparticles supported on activated carbon prepared by aqueous hydrazine reduction, J. Colloid Interf. Sci. 299 (2006) 238–248.
[15] E.-J. Shin, M.A. Keane, Gas phase catalytic hydrodechlorination of chlorophenols using a supported nickel catalyst, Appl. Catal. B: Environ. 18 (1998) 241–250.
[16] M.A. Keane, G. Pina, G. Tavoularis, The catalytic hydrodechlorination of mono-, di- and trichlorobenzenes over supported nickel, Appl. Catal. B: Environ. 48 (2004) 275–286.
[17] S.-F. Cheng, S.-C. Wu, The enhancement methods for the degradation of TCE by zero-valent metals, Chemosphere 41 (2000) 1263–1270.
[18] S.-F. Cheng, S.-C. Wu, Feasibility of using metals to remediate water containing TCE, Chemosphere 43 (2001) 1023–1028.

[19] B. Schrick, J.L. Blough, A.D. Jones, T.E. Mallouk, Hydrodechlorination of trichloroethylene to hydrocarbons using bimetallic nickel–iron nanoparticles, Chem. Mater. 14 (2002) 5140–5147.
[20] W.-X. Zhang, C.-B. Wang, H.-L. Lien, Treatment of chlorinated organic contaminants with nanoscale bimetallic particles, Catal. Today 40 (1998) 387–395.
[21] D.G. Crosby, Environmental chemistry of pentachlorophenol, Pure Appl. Chem. 53 (1981) 1051–1080.
[22] R. Chetty, P.A. Christensen, B.T. Golding, K. Scott, Fundamental and applied studies on the electrochemical hydrodehalogenation of halogenated phenols at a palladised titanium electrode, Appl. Catal. A: Gen. 271 (2004) 185–194.
[23] A. Vallecillo, P.A. Garcia-Encina, M. Pena, Anaerobic biodegradability and toxicity of chlorophenols, Water Sci. Technol. 40 (1999) 161–168.
[24] J. Dolfing, B.K. Harrison, Gibbs free energy of formation of halogenated aromatic compounds and their potential role as electron acceptor in anaerobic environments, Environ. Sci. Technol. 26 (1992) 2213–2216.
[25] G.N. Glavee, K.J. Klabunde, C.M. Sorensen, G.C. Hadjipanayis, Chemistry of borohydride reduction of iron(III) ions in aqueous and nonaqueous media-formation of nanoscale Fe, FeB and Fe_2B powders, Inorg. Chem. 34 (1995) 28–35.
[26] H.L. Lien, W.X. Zhang, Nanoscale iron particles for complete reduction of chlorinated ethenes, Colloids Surf. A 119 (2001) 97–105.
[27] W. Zhou, L. He, R. Cheng, L. Guo, C.P. Chen, J.L. Wang, Synthesis of Ni nanochains with various sizes: the magnetic and catalytic properties, J. Phys. Chem. C 113 (2009) 17355–17358.
[28] S. Choe, Y.Y. Chang, K.Y. Hwang, J. Khim, Kinetics of reductive denitrification by nanoscale zero-valent iron, Chemosphere 41 (2000) 1307–1311.
[29] M. Zielinski, R. Wojcieszak, S. Monteverdi, M. Mercy, M.M. Bettahar, Hydrogen storage on nickel catalysts supported on amorphous activated carbon, Catal. Commun. 6 (2005) 777–783.
[30] M.O. Nutt, J.B. Hughes, M.S. Wong, Designing Pd-on-Au bimetallic nanoparticles catalysts for trichloethene hydrodechlorination, Environ. Sci. Technol. 39 (2005) 1346–1353.
[31] T.T. Lim, J. Feng, B.W. Zhu, Kinetic and mechanistic examinations of reductive transformation pathways of brominated methanes with nano-scale Fe and Ni/Fe particles, Water Res. 41 (2007) 875–883.
[32] R. Cheng, J.L. Wang, W.X. Zhang, Comparison of reductive dechlorination of p-chlorophenol using Fe^0 and nanosized Fe^0, J. Hazard. Mater. 144 (2007) 334–339.
[33] Y.H. Tee, E. Grulke, D. Bhattacharyya, Role of Ni/Fe nanoparticle composition on the degradation of trichloroethylene from water, Ind. Eng. Chem. Res. 44 (2005) 7062–7070.
[34] Y. Park, K.M. Knowles, Particle-size effect on the ferroelectric phase transition in $PbSc_{1/2}Ta_{1/2}O_3$ ceramics, J. Appl. Phys. 83 (11) (1998) 5702–5708.
[35] Y.F. Yang, Y.H. Zhou, Particle size effects for oxygen reduction on dispersed silver + carbon electrodes in alkaline solution, J. Electroanal. Chem. 397 (1995) 271–278.
[36] V.M. Mastikhin, S.N. Goncharova, V.M. Tapilin, V.V. Terskikh, B.S. Balzhinimaev, Effect of particle size upon catalytic and electronic properties of supported Ag catalysts: combined catalytic, ^{109}Ag NMR and quantum chemistry studies, J. Mol. Catal. A: Chem. 96 (1995) 175–179.
[37] W.J. Plieth, Electrochemical properties of small clusters of metal atoms and their role in surface enhanced Raman scattering, J. Phys. Chem. 86 (1982) 3166–3170.
[38] K.A. Friedrich, F. Henglein, U. Stimming, W. Unkauf, Size dependence of the CO monolayer oxidation on nanosized Pt particles supported on gold, Electrochim. Acta 45 (2000) 3283–3293.
[39] Y. Takasu, X.G. Zhang, S. Minoura, Y. Murakami, Size effects of ultrafine palladium particles on the electrocatalytic oxidation of CO, Appl. Surf. Sci. 121–122 (1997) 596–600.
[40] R. Cheng, J.L. Wang, Degradation of chlorinated phenols by nanoscale zero-valent iron, Front. Environ. Sci. Eng. Chin. 2 (2008) 103–108.
[41] B.A. Manning, M.L. Hunt, C. Amrhein, J.A. Yarmoff, Arsenic(III) and arsenic(V) reactions with zerovalent iron corrosion products, Environ. Sci. Technol. 36 (2002) 5455–5461.
[42] S.R. Kanel, B. Manning, L. Charlet, H. Choi, Removal of arsenic(III) from groundwater by nanoscale zero-valent iron, Environ. Sci. Technol. 39 (2005) 1291–1298.
[43] B. Gu, T.J. Phelps, L. Liang, M.J. Dickey, Y. Roh, B.L. Kinsall, A.V. Palumbo, G.K. Jacobs, Biogeochemical dynamics in zero-valent iron columns: implications for permeable reactive barriers, Environ. Sci. Technol. 33 (1999) 2170–2177.